COMPRESSION BEHAVIOR OF ANNULAR ELASTIC LAYERS BONDED BETWEEN RIGID PLATES

H.-C. Tsai *

Department of Construction Engineering
National Taiwan University of Science and Technology
Taipei, Taiwan 10607, R.O.C.

ABSTRACT

An annular elastic layer bonded between rigid plates and subjected to a compressive force normal to the layer is analyzed through a theoretical approach. On the basis of two kinematic assumptions, the governing equation for the mean pressure is established from the equilibrium equation, which is then solved by satisfying the stress boundary conditions. Through the obtained pressure expression, the compression stiffness of the bonded annular layer is derived in closed form and is very close to the finite element solution. The derived formula has no limitation on the Poisson's ratio and is more concise than the previous research. Through the asymptotic approach, the compression stiffness for the incompressible elastic layers is derived and is more accurate than the previous research obtained by directly neglecting the bulk compressibility. The stiffness reduction caused by the central hole is more prominent when the Poisson's ratio is close to 0.5.

Keywords: Bonded elastic layer, Elastomeric bearing, Seismic isolation.

1. INTRODUCTION

A laminated elastomeric bearing consists of elastomeric layers bonded to interleaving reinforcing sheets. The high stiffness of the reinforcements restrains the lateral expansion of elastomeric layers and results in higher stiffness than an unbonded elastomeric layer in the vertical direction normal to the layers. Employed in many fields, such as seismic isolation, laminated elastomeric bearings can provide high vertical rigidity to sustain gravity loading, while still providing the same horizontal flexibility of an unbonded elastomer to reduce the seismic response of buildings.

The simplest approach to derive the compression stiffness of the bonded elastic layer assumes the elastomeric layer is an incompressible material [1]. For nearly incompressible materials, such as rubber, the assumption of complete incompressibility tends to overestimate the compression stiffness of the bonded rubber layer when the shape factor of the bonded layer (defined as the ratio of the one bonded area to the force-free area) is high. The "approximate pressure solution" approach which includes the effect of bulk compressibility can overcome this problem [2]. The compression stiffness obtained through the pressure approach developed by Tsai and Lee [3] is suitable for materials of any Poisson's ratio.

Pinarbasi *et al*. [4] employed the approximate theory to derive the compression stiffness of the boned circular layers. They found that the formulas derived by the zero order theory and the first order theory are the same as the formula obtained by Tsai and Lee [3]. Pinarbasi *et al*. [4] also derived the compression stiffness of the bonded annular layers by using the first order theory, but the proposed approximate theory seems too complicated to follow. Constantinou *et al*. [5] applied the "approximate pressure solution" approach to derive the compression stiffness of hollow-circular bearings. However, the "approximate pressure solution" approach is accurate only for the bearings of a high shape factor and a Poisson's ratio between 0.49 and 0.5 [3]. The compression stiffness of the bonded annular rubber block presented by Ling *et al*. [6] is valid only for incompressible materials. Ling [7] derived the compression stiffness of thin annular disks of compressible materials by the perturbation-Ritz method, but did not present the formula explicitly because it is "too lengthy".

In this paper, the pressure approach developed by Tsai and Lee [3] for the compression stiffness of the bonded circular layers is extended to analyze the compression stiffness of the bonded annular layers. The pressure approach adopts two kinematic assumptions on the bonded elastic layers: (i) planes parallel to the rigid bonding plates before deformation remain planar after loading; (ii) lines normal to the rigid bonding plates

* Corresponding author (hctsai@mail.ntust.edu.tw)

DOI : 10.1017/jmech.2012.107
Copyright © 2012 The Society of Theoretical and Applied Mechanics, R.O.C.
https://doi.org/10.1017/jmech.2012.107 Published online by Cambridge University Press

before deformation become parabolic after loading. The mean pressure is determined from the equilibrium equation by satisfying the stress boundary conditions of the bonded layers. The compression stiffness of annular bearings is then derived and compared with the finite element solution and the previously published formulae.

2. SOLUTION FOR THE PRESSURE

An annular layer of linear elastic, homogeneous and isotropic material bonded between two rigid plates, shown in Fig. 1, has outer diameter $2b$, inner diameter $2a$ and thickness t. A cylindrical coordinate system (r, θ, z) is established with the origin at the center of the layer. Under the compression force P, the elastic layer is in the axisymmetric stress state so the displacement in the θ direction vanishes. When the thickness of the elastic layer is much smaller than the outer diameter, the displacements in the r and z directions, denoted as u and w respectively, can be assumed as

$$u(r,\, z) = \bar{u}(r)\left(1-\frac{4z^2}{t^2}\right) \tag{1}$$

$$w(r,\, z) = \bar{w}(z) \tag{2}$$

where $\bar{u}$ is the horizontal displacement in the middle plane of the layer. Equation (1) represents the kinematic assumption of quadratic-varied displacement which simulates the lateral bulging of the elastic layer created by the compression force. Equation (2) represents the assumption that planes parallel to the plates remain planar.

The effective pressure $\bar{p}$ is the average of the mean pressure p through the thickness, defined as

$$\bar{p}(r) = \frac{1}{t}\int_{-t/2}^{t/2} p(r,\, z)\, dz = -\frac{1}{t}\int_{-t/2}^{t/2} \kappa(u_{,r} + \frac{u}{r} + w_{,z})\, dz \tag{3}$$

where the commas imply partial differentiation with respect to the indicated coordinate, and κ is the bulk modulus. By applying the assumptions in Eqs. (1) and (2), (3) becomes

$$\frac{\bar{p}}{\kappa} = \varepsilon_c - \frac{2}{3}\left(\bar{u}_{,r} + \frac{\bar{u}}{r}\right) \tag{4}$$

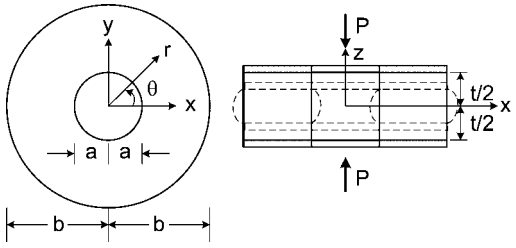


Fig. 1 Annular elastic layer bonded between rigid plates under compression load

where ε_c is the effective compression strain defined as

$$\varepsilon_c = -\frac{1}{t}\left[\bar{w}(t/2) - \bar{w}(-t/2)\right] \tag{5}$$

Substitution of the displacement assumptions in Eqs. (1) and (2) into the equilibrium equation in the r direction and integration of the resulting equation through the thickness of the layer lead to [3]

$$\bar{u} = -\frac{3}{2\alpha^2}\frac{\bar{p}_{,r}}{\kappa} \tag{6}$$

where α is equal to the parameter $\bar{\alpha}$ used by Tsai and Lee [3]. In terms of Poisson's ratio of the elastic layer, v, it has a form as

$$\alpha = \sqrt{\frac{6(1-2\nu)}{t^2(1-\nu)}} \tag{7}$$

The governing equation for the effective pressure can be derived by substituting Eq. (6) into Eq. (4),

$$\bar{p}_{,rr} + \frac{1}{r}\bar{p}_{,r} - \alpha^2\bar{p} = -\alpha^2\kappa\varepsilon_c \tag{8}$$

The normal stress in the r direction, σ_r, and the mean pressure have the following relation

$$\sigma_r = \frac{E}{1+\nu}\left(-\frac{\nu}{(1-2\nu)\,\kappa}p + u_{,r}\right) \tag{9}$$

with E being the elastic modulus of the layer. By integrating the above equations through the thickness of the elastic layer and applying Eqs. (1), (4) and (6), the boundary conditions $\sigma_r\,(b,\, z) = 0$ and $\sigma_r\,(a,\, z) = 0$ become

$$\frac{1}{b}\bar{p}_{,r}(b) - \frac{6}{t^2}\bar{p}(b) = -\alpha^2\kappa\varepsilon_c \tag{10}$$

$$\frac{1}{a}\bar{p}_{,r}(a) - \frac{6}{t^2}\bar{p}(a) = -\alpha^2\kappa\varepsilon_c \tag{11}$$

The effective pressure can be solved from Eq. (8) by satisfying the conditions in Eqs. (10) and (11),

$$\bar{p}(r) = \kappa\varepsilon_c\left\{1 - \frac{\nu}{(1-\nu)}\frac{\alpha b}{\Lambda}\left[\left(h_K(a) - \frac{a}{b}h_K(b)\right)I_0(\alpha r) - \left(h_I(a) - \frac{a}{b}h_I(b)\right)K_0(\alpha r)\right]\right\} \tag{12}$$

where I_n and K_n are the modified Bessel functions of the first and second kinds, respectively, of order n; h_I and h_K are the functions defined as

$$h_I(r) = \alpha r\, I_0(\alpha r) - \frac{(1-2\nu)}{(1-\nu)}I_1(\alpha r) \tag{13}$$

$$h_K(r) = \alpha r\, K_0(\alpha r) + \frac{(1-2\nu)}{(1-\nu)}K_1(\alpha r) \tag{14}$$

and Λ is

$$\Lambda = h_I(b)\, h_K(a) - h_I(a)\, h_K(b) \tag{15}$$

https://doi.org/10.1017/jmech.2012.107 Published online by Cambridge University Press

3. COMPRESSION STIFFNESS

The compression stiffness of the bonded annular layers is determined by the effective compression modulus defined as

$$E_c = \frac{P}{\pi(b^2 - a^2)\,\varepsilon_c} = \frac{-\int_0^{2\pi}\int_a^b \bar{\sigma}_z\, r dr d\theta}{\pi(b^2 - a^2)\,\varepsilon_c} \tag{16}$$

where the effective vertical stress $\bar{\sigma}_z$ is the average of the vertical stress σ_z through the thickness of the layer,

$$\bar{\sigma}_z = \frac{1}{t}\int_{-t/2}^{t/2} \sigma_z\, dz = -\frac{E}{(1+\nu)}\left(\frac{\nu}{(1-2\nu)}\frac{1}{\kappa}\bar{p} + \varepsilon_c\right) \tag{17}$$

Substituting Eq. (12) into Eq. (17) and using the following Wronskian equation [8]

$$I_0(x)K_1(x) + I_1(x)K_0(x) = \frac{1}{x} \tag{18}$$

the effective compression modulus of the bonded annular layers can be derived as

$$\frac{E_c}{E} = \frac{1}{1+\nu}\left[1 + \frac{\nu}{1-2\nu}\left(1 - \frac{1}{\left[1-(a/b)^2\right]}\frac{2\nu}{(1-\nu)}\frac{1}{\Lambda}\left[H_1 + (a/b)^2 H_2 - 2(a/b)\right]\right)\right] \tag{19}$$

where

$$H_1 = h_K(a)I_1(\alpha b) + h_I(a)K_1(\alpha b) \tag{20}$$

$$H_2 = h_K(b)I_1(\alpha a) + h_I(b)K_1(\alpha a) \tag{21}$$

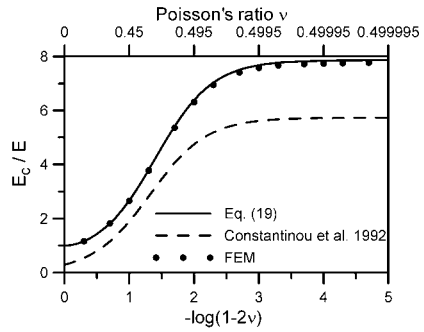
The effective compression stiffness in Eq. (19) would be equivalent to the formula derived by Pinarbasi *et al*. [4], if the sign between the two terms in the brace of Eq. (42) presented in the paper of Pinarbasi *et al*. [4] was changed from negative to positive. This sign difference could be a typographical error, but it is not verified because of the complicated approximate theory. Mathematically, the compression modulus in Eq. (19) is the same as the *corrected* formula derived by Pinarbasi *et al*. [4], but the expression in Eq. (19) is more concise because of using the Wronskian equation in Eq. (18).

The normalized compression modulus in Eq. (19) is a function of Poisson's ratio v, radius ratio a/b and shape factor S which is defined as

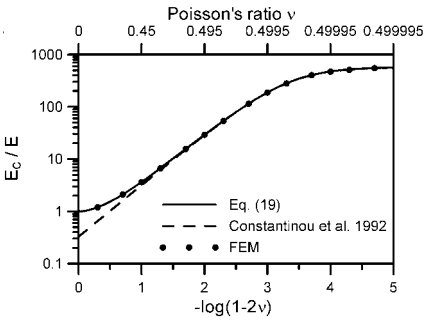
$$S = \frac{b}{2t}\left(1 - \frac{a}{b}\right) \tag{22}$$

for the bonded annular layers. The normalized compression modulus in Eq. (19) is plotted in Fig. 2 as a function of v for the layers of S = 2 and S = 20 with a/b = 0.1.

Figure 2 also depicts the result of the finite element analysis. The axisymmetric eight-node isoparametric



(a) S = 2, a/b = 0.1



(b) S = 20, a/b = 0.1

Fig. 2 Compression modulus of bonded annular layers varied with Poisson's ratio

elements in the computer program SAP2000 [9] are used in the finite element models. Due to symmetric loading, only the upper half of the elastic layer needs to be modeled. Simulating the middle plane of the elastic layer, the nodes at the bottom line of the model are restrained in the vertical direction but allowed to move in the radial direction. The nodes at the top line of the model are restrained in the vertical and radial directions to simulate the restraint of the rigid plate, but are subjected to a prescribed downward displacement. The vertical load applied to the elastic layer is calculated by summing up the vertical reactions. There are four layers of finite element mesh in the vertical direction. The division of finite element mesh in the radial direction is dependent on keeping the element shapes as close to a square as possible. The finite element solution is very close to the theoretical solution, which indicates that the two kinematic assumptions used in the pressure approach are acceptable for the compression stiffness of the bonded elastic layers.

The solution derived through the "approximate pressure solution" approach by Constantinou *et al*. [5] is also plotted in Fig. 2, which has a typing error in the original paper and has been corrected here. The plot reveals that the "approximate pressure solution" approach is accurate only when the shape factor is high and the Poisson's ratio is near 0.5, and the derived compression modulus cannot converge to the elastic modulus of the layers when the Poisson's ratio becomes zero.

When the layer's material becomes incompressible, $v \to 0.5$ and $\alpha \to 0$. Substituting the following series forms of the modified Bessel functions [8] into Eq. (19),

https://doi.org/10.1017/jmech.2012.107 Published online by Cambridge University Press

$$I_0(x)=1+\frac{1}{4}x^2+\frac{1}{64}x^4+\cdots \tag{23}$$

$$I_1(x)=\frac{1}{2}x+\frac{1}{16}x^3+\frac{1}{384}x^5+\cdots \tag{24}$$

$$K_0(x)=-I_0(x)\ln\left(\frac{x}{2}\right)-\gamma+\frac{1-\gamma}{4}x^2+\frac{3-2\gamma}{128}x^4+\cdots \tag{25}$$

$$K_1(x)=I_1(x)\ln\left(\frac{x}{2}\right)+\frac{1}{x}-\frac{1-2\gamma}{4}x-\frac{5-4\gamma}{64}x^3+\cdots \tag{26}$$

where $\gamma = 0.5772$ is Euler's constant, and neglecting the high order terms of α, the asymptotic solution of Eq. (19) for $v \to 0.5$ can be derived as

$$\frac{E_{ci}}{E}=1+\frac{2S^2}{\left(1-\frac{a}{b}\right)^2}\left(1+(a/b)^2-\frac{24S^2(a/b)^2}{\left(1-\frac{a}{b}\right)^2-24S^2\frac{(a/b)^2}{\left[1-(a/b)^2\right]}\ln\left(\frac{a}{b}\right)}\right) \tag{27}$$

which is the effective compression modulus of incompressible materials, denoted as E_{ci}. If the shape factor $S >> 1$, Eq. (27) can be approximated as

$$\frac{E_{ca}}{E}\approx\frac{2S^2}{(1-a/b)^2}\left(1+(a/b)^2+\frac{1-(a/b)^2}{\ln(a/b)}\right) \tag{28}$$

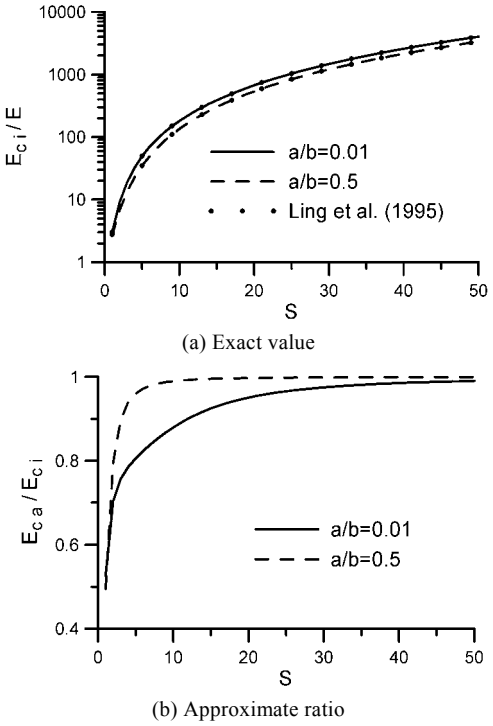
which is the solution presented by Constantinou *et al.* [5] for the compression modulus of incompressible materials, denoted as E_{ca}.

Figure 3(a) plots the curves of E_{ci} as a function of S for $a/b = 0.01$ and $a/b = 0.5$, which indicates that the compression modulus of incompressible materials increases with increasing shape factor or decreasing radius ratio. Figure 3(a) also depicts the compression stiffness of an incompressible material obtained by Ling *et al.* [6] through the variation approach, which is very close to the curves calculated by Eq. (27). The ratio of the approximate solution E_{ca} in Eq. (28) to the exact solution E_{ci} in Eq. (27) is plotted in Fig. 3(b), which shows that the approximate solution has a larger error for a smaller shape factor or a smaller radius ratio.

The compression modulus of the bonded full-circular layers, E_{cf}, is the asymptotic solution of Eq. (19) for $a \to 0$. Using Eqs. (23) ~ (26), it can be found that

$$\frac{E_{cf}}{E}=\frac{1}{1+\nu}\left[1+\frac{\nu}{1-2\nu}\left(1-\frac{2\nu}{(1-\nu)}\frac{I_1(\alpha b)}{h_I(b)}\right)\right] \tag{29}$$

which is the same solution presented by Tsai and Lee [3]. Figure 3(a) shows that, under the same shape factor S, the compression modulus does not have a significant difference between $a/b = 0.01$ and $a/b = 0.5$. This is because the shape factor is also a linear function of the radius ratio as shown in Eq. (22). The same



(a) Exact value

(b) Approximate ratio

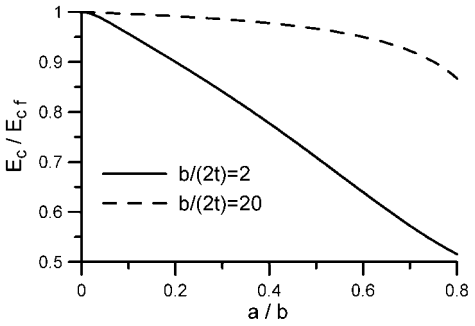
Fig. 3 Compression modulus of bonded annular layers varied with shape factor for incompressible elastic material

shape factor means the layers of larger a/b have a larger b/t ratio. To study the effect of a central hole on the compression stiffness, Fig. 4 plots the normalized compression modulus under the same values of $b/(2t)$, which is the shape factor of the bonded full-circular layers. For $v = 0.45$, the thicker layer has more stiffness reduction by the central hole under the same outer radius. But for $v = 0.49995$, the thinner layer has more stiffness reduction by the central hole under the same outer radius. The stiffness reduction caused by the central hole is more prominent when the Poisson's ratio is close to 0.5.

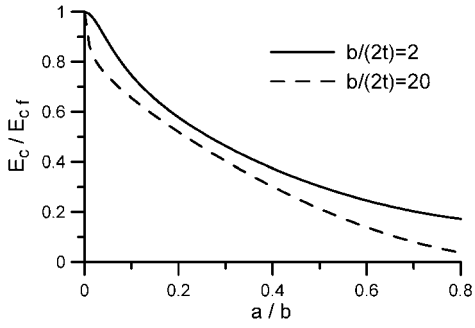
4. DISPLACEMENT AND STRESS DISTRIBUTION

By using the pressure solution in Eq. (12), the effective vertical stress in Eq. (17) can be derived. The effective vertical stress normalized by the average compression stress $E_c \varepsilon_c$ is plotted in Fig. 5 as a function of r/b. The figure shows that the vertical stress is uniformly distributed in the layers of small Poisson's ratio ($v = 0.45$) and large shape factor ($S = 20$). The distribution of vertical stress is symmetrical to the middle point of annular thickness for the layers of large radius ratio ($a/b = 0.5$), but is more concentrated in the inner edge for the layers of small radius ratio ($a/b = 0.01$). The vertical stress in the middle plane of the layer calculated by the finite element method is also plotted in the figure and matches the theoretical solution except near the inner and outer edges.

https://doi.org/10.1017/jmech.2012.107 Published online by Cambridge University Press



(a) $v = 0.45$



(b) $v = 0.49995$

Fig. 4 Normalized compression modulus varied with radius ratio under the fixed ratio of outer radius to thickness

Using the solution of the effective pressure in Eq. (12), the radial displacement in the middle plane can be found from Eq. (6),

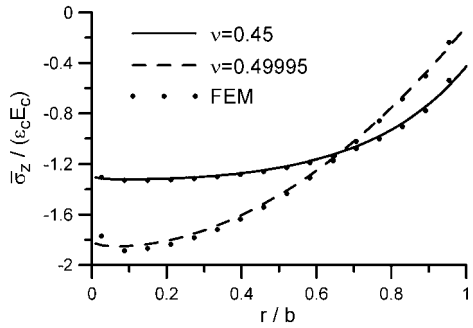
$$\bar{u}(r) = \varepsilon_c\, b \frac{3}{2} \frac{\nu}{(1-\nu)} \frac{1}{\Lambda} \left[\left(h_K(a) - \frac{a}{b} h_K(b) \right) I_1(\alpha r) + \left(h_I(a) - \frac{a}{b} h_I(b) \right) K_1(\alpha r) \right] \tag{30}$$

Substituting this into Eq. (1) leads to the same expression of the displacement in the r direction derived by Pinarbasi *et al*. [4]. The shear strain in the bonded surface between the elastic layer and the rigid plates, which represents the magnitude of shear traction on the elastic layer, is related to the function $\bar{u}(r)$ by

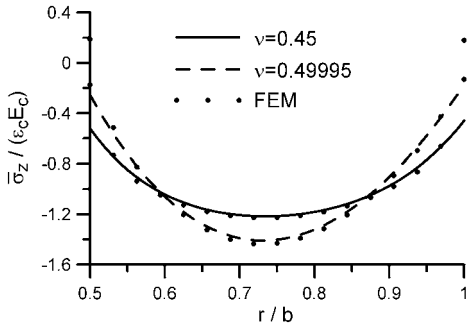
$$\gamma_{rz}(r,\ t/2) = u_{,z}(r,\ t/2) = -\frac{4}{t}\bar{u}(r) \tag{31}$$

The radial displacement in the middle plane calculated from Eq. (30) is compared with the finite element solution in Figure 6, indicating that both solutions are very close. For the high shape factor (S = 20), the function $\bar{u}(r)$ is almost linearly varied in the case of a large hole (a/b = 0.5), but becomes sharply increased in the inner edge for the case of a very small hole (a/b = 0.01). This means very high shear traction is generated near the inner edge of the bounded surface.

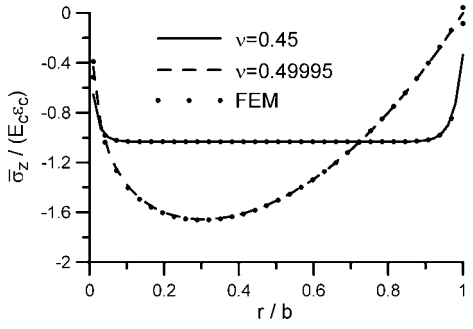
Calculated from Eq. (1), the radial displacements varied along the thickness of the layer at the inner and outer edges and the middle between the edges ($r = (a + b)/2$) are plotted in Fig. 7. The theoretical solution



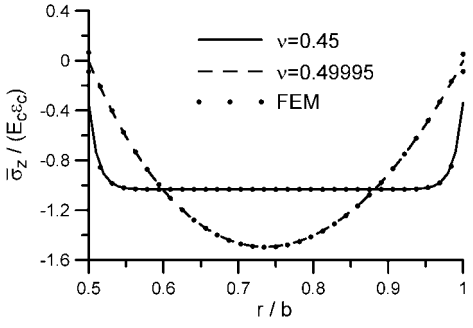
(a) $a/b = 0.01$, $S = 2$



(b) $a/b = 0.5$, $S = 2$



(c) $a/b = 0.01$, $S = 20$



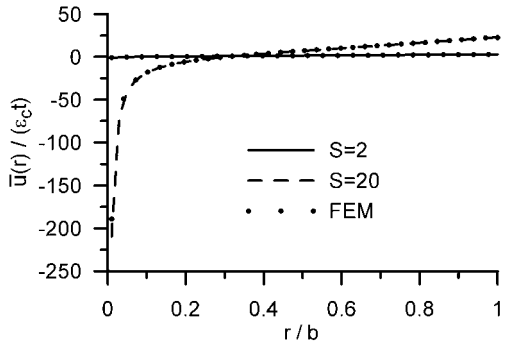
(d) $a/b = 0.5$, $S = 20$

Fig. 5 Distribution of normalized vertical stress along radius

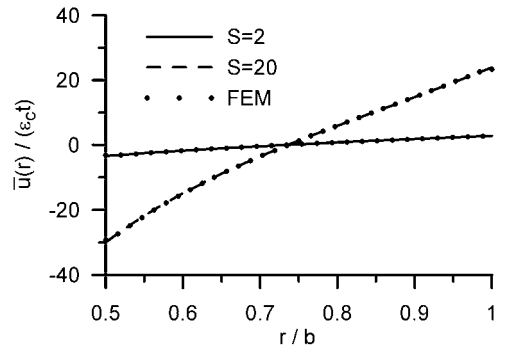
is close to the finite element solution, which indicates that the kinematic assumption of quadratic-varied displacement in Eq. (1) is reasonable.

The distribution of the shear stress in the bonded surface, $\tau_{rz}(r, t/2)$, normalized to the average vertical stress $E_c\,\varepsilon_c$ is plotted in Figure 8 for the radius ratio a/b = 0.1. The theoretical solution matches very well with the finite element solution except at places near the inner and outer edges.

https://doi.org/10.1017/jmech.2012.107 Published online by Cambridge University Press

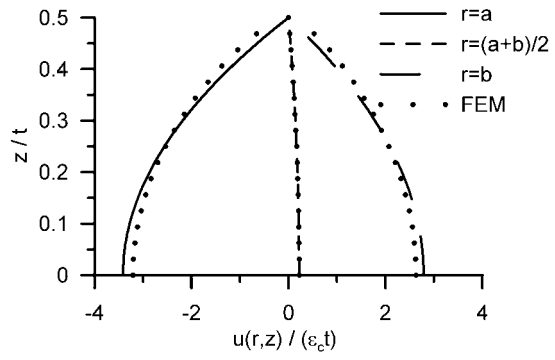


(a) $a/b = 0.01$, $v = 0.49995$

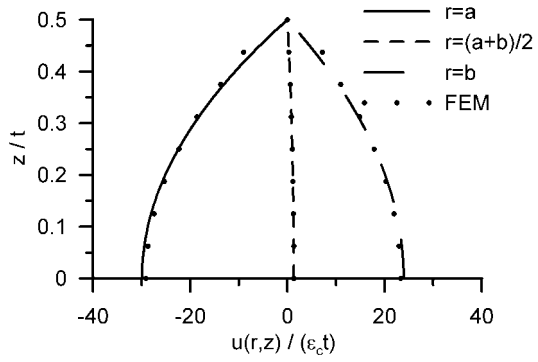


(b) $a/b = 0.5$, $v = 0.49995$

Fig. 6 Radial displacement in middle plane varied along radius

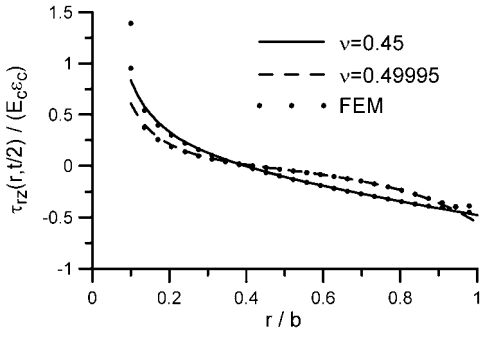


(a) $a/b = 0.5$, $S = 2$, $v = 0.49995$

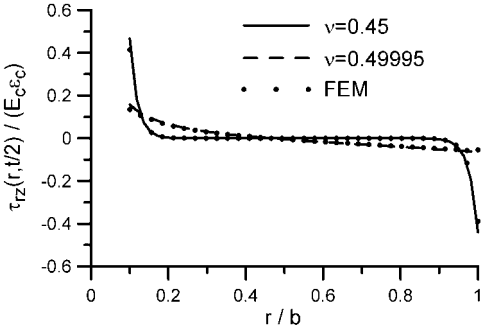


(b) $a/b = 0.5$, $S = 20$, $v = 0.49995$

Fig. 7 Radial displacement varied along thickness



(a) $a/b = 0.1$, $S = 2$



(b) $a/b = 0.1$, $S = 20$

Fig. 8 Distribution of normalized bonding shear stress along radius

5. CONCLUSIONS

On the basis of the two kinematic assumptions, *i.e.* horizontal planes remain planar and vertical lines become parabolic after deformation, the compression stiffness of the annular elastic layers bonded between rigid plates has been derived through the pressure approach. The derived formula has no limitation on the Poisson's ratio and is more concise than the previous research. For elastic layers of incompressible material, the compression stiffness has been derived through the asymptotic approach, which provides a more accurate solution. The solution of the previous research, by directly neglecting the bulk compressibility, is accurate only when the shape factor is large.

While the compression stiffness of the bonded annular layers can be determined by the finite element method, the closed-form solution provides an easier way to calculate the compression stiffness of the bonded annular layers under any configuration. The closed-form solutions for the stiffness and stress distribution are very close to the finite element solutions except the stress near the inner and outer edges.

ACKNOWLEDGMENTS

The National Science Council of Taiwan supported the research work reported in this paper under Grant No. NSC96-2211-E011-044. This support is greatly appreciated.

https://doi.org/10.1017/jmech.2012.107 Published online by Cambridge University Press

REFERENCES

1. Gent, A. N. and Lindley, P. B., "The Compression of Bonded Rubber Blocks," *Proceeding of the Institution of Mechanical Engineers*, **173**, pp. 111–117 (1959).
2. Kelly, J. M., *Earthquake-Resistant Design with Rubber*, 2nd Ed., Springer-Verlag, London (1997).
3. Tsai, H.-C. and Lee, C.-C., "Compressive Stiffness of Elastic Layers Bonded between Rigid Plates," *International Journal of Solids and Structures*, **35**, pp. 3053–3069 (1998).
4. Pinarbasi, S., Mengi, Y. and Akyuz, U., "Compression of Solid and Annular Circular Discs Bonded to Rigid Surfaces," *International Journal of Solids and Structures*, **45**, pp. 4543–4561 (2008).
5. Constantinou, M. C., Kartoum, A. and Kelly, J. M., "Analysis of Compression of Hollow Circular Elastomeric Bearings," *Engineering Structures*, **14**, pp. 103–111 (1992).
6. Ling, Y., Engel, P. A. and Brodsky, W. L., "Compression of Bonded Annular Rubber Blocks," *Journal of Engineering Mechanics*, ASCE, **121**, pp. 661–666 (1995).
7. Ling, Y., "An Approximate Solution for the Compression of a Bonded Thin Annular Disk," *Journal of Applied Mechanics*, ASME, **63**, pp. 780–787 (1996).
8. Abramowitz, M. and Stegun, I. A., *Handbook of Mathematical Functions with Formulas*, *Graphs and Mathematical Tables*, Dover, New York (1972).
9. SAP2000 – Integrated Structural Analysis & Design Software, Computers and Structures Inc., Berkeley, California (1997).

(Manuscript received September 29, 2011,
accepted for publication February 20, 2012.)

https://doi.org/10.1017/jmech.2012.107 Published online by Cambridge University Press